



Density Function Theory Study of the Physicochemical Characteristics of 2-nitrophenol

Rebaz Obaid Kareem^{a*}, Othman Abdulrahman Hamad^b, Omer Kaygili^c

^a Physics Department, College of Science, University of Halabja, 46018, Halabja, Iraq

^b University of Raparin, College of Science, Department of Chemistry, Sulamani, Iraq

^c Department of Physics, Faculty of Science, Firat University, 23119, Elazig, Türkiye

* Corresponding author: E-mail: obedrebaz9@gmail.com

ABSTRACT

2-Nitrophenol (2-NP) is utilized in the production of bio-refractory organic compounds, and petrochemicals, and in the synthesis of many drugs and weed killers. The chemical structure of 2-NP is $C_6H_5NO_3$. The structure of 2-NP is important as the nitro group (NO_2). In this present investigation, the Gaussian 5.0 program was used to compute the difference in energy level that exists between the HOMO and LUMO states of the BGs. This information was then used to optimize the shape of the 2-NP structures using DFT methods. The 3-21G/B3LYP base set has a minimum value for the BG energy of 3.48 eV. This is the minimum value that can be achieved. The DOS for 2-NP was measured to have its maximum possible value of 2.23 eV/atom. According to the results of the IR, and Raman spectrum, the C-H stretching vibration peak for 2-NP was found to be between 3208.96 cm^{-1} and 3243.76 cm^{-1} . The maximum excitation energy was analyzed at a wavelength of 382.1 nm, and the oscillator strength was determined at 0.0537 UV Spectroscopy. In the potential energy map (PE), the colors are changed from blue to red in the range of $-4.442e^{-2}$ to $4.442e^{-2}$.

ARTICLE INFO

Keywords:

Density Function Theory (DFT)
HOMO-LUMO
The density of State (DOS)
IR, Raman spectrum
UV spectroscopy
Potential Energy (PE) map

Received: 2023-03-30

Accepted: 2023-06-02

ISSN: 2651-3080

DOI: 10.54565/jphcfum.1273771

1. INTRODUCTION

A nitroaromatic chemical derivative of phenol is 2-nitrophenol (2-NP). It is obtained through phenol nitration and has been synthesized with high yields by neutralization reactions [1]. The structure of 2-NP is important as the nitro group (NO_2) has a strong electronegativity and pulls electrons away from the aromatic rings [2]. 2-NP make excellent electron acceptors because their electron-absorbing groups have been replaced [3]. There was an appropriate intramolecular hydrogen bonding between ortho groups, so a decrease in the boiling and melting points were associated with the bonding [4]. 2-NP can be detected by a peak at 415 nm in the UV-vis spectrum [5]. 2-NP isomers are water soluble as a result of dissociation and are somewhat acidic in water [2, 6]. When a 2-NP solution has a pH higher than (7.17), the molecules are mostly deprotonated (negatively charged), but when the pH is lower than 7, molecules are in their molecular state. The presence of nitro-group on the ring's made it have the ability to remove electrons, 2-NP is not positively charged at the low pH of the solution. Even though the pH of the solution is lower than 4, 2-NP will engage hydrophobically and form hydrogen bonds with oxygenated groups that have lone electron pairs in the adsorbents when combined with the OH of the aromatic rings [7]. When the OH molecule is hydrogen bridge free,

the expected rotation barrier is between (16.98-17.8) kJ/mol; if the NO_2 molecule is involved in a single hydrogen bond, the calculated rotation barrier is about 69 kJ/mol; and if the nitro molecule is simultaneously involved in two hydrogen bonds, the predicted rotation barrier is 93.3 kJ/mol. As a result, the energy compound and molecules take on various values depending on whether a non-planar or planar reference structure is utilized [8].

Nitrophenol and its derivatives are used in the manufacture of bio refractory organic compounds, petrochemicals, pharmaceuticals (e.g., acetaminophen), pesticides (e.g. methyl and ethyl parathion), leather treatment, for military purposes [9-11], in the synthesis of many drugs, weed killers [12], insecticides, pesticides, synthetic dyes [4, 13], textiles [14]. Since 2-NP is widely employed in the manufacturing of pharmaceuticals, including antipyretic and analgesic treatments, the reduction of 2-NP to 2-aminophenol (2-AP) is a very beneficial chemical process [5]. One of the most potent explosives used to create lethal weapons is nitroarenes, 2,4,6-trinitrophenol (TNP), which has explosive properties and is a key ingredient in rocket fuel, fireworks, and analytical reagents [3].

The wastewater from these industries contains phenolic residues and their derivatives, which can have negative effects on both the environment and human

health. It is highly toxic and one of the most dangerous pollutants [2, 12]. It was discovered to be more hazardous [7]. Numerous industrial wastes that contaminate the soil, groundwater, and vegetation contain it [3]. The US Environmental Protection Agency (EPA) states that nitrophenol's maximum containment values range from 0.01 to 2.0 μgL^{-1} [7, 9, 15]. Due to its harmful effects on human health, including cancer, liver damage, kidney failure, and blood disorders, the US EPA has listed 2-NP as one of the "priority pollutants" (oxygen-deficient hemoglobin) [16].

2-NP is extremely toxic to the systems of living things; therefore, it is crucial to develop a quick, accurate, and useful method to determine it [6]. So far, numerous analytical techniques, including chromatography, electrophoresis [5][d], fluorescence [16], spectrometry, UV-vis spectroscopy [17], pencil graphite electrode [6], and electrochemical, have been improved to determine 2-NP. Among the mentioned methods, the electrochemical methods can be preferred due to their simple operation, low cost, rapid analysis, and more sensitive results, as well as a modified glassy carbon electrode (GCE) used to determine 2-NP. Although, these non-biodegradable organic contaminants have been removed or transformed into useful chemicals using a variety of chemical processes, such as wet oxidation, coagulation, adsorption, catalytic oxidation, and ozonation [18].

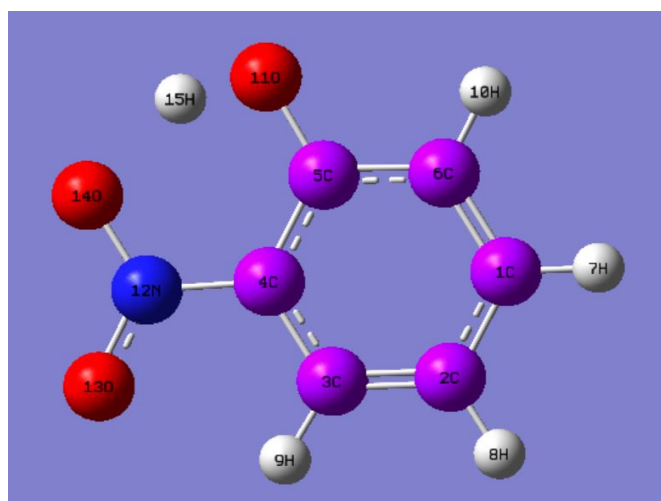


Figure 1 Geometry Optimization 2-NP

2. MATERIAL AND METHOD

The software program Gaussian 5.0.9W was used to do all of the necessary atomic computations and simulations in the three-dimensional form of the molecule components in the gas phase [19, 20]. To determine the initial geometries of the compounds, the software known as Gauss View 5.0 package was utilized, and the Gaussian 09W was utilized for output computations. Since the DFT method takes into account the density of electrons, it can generate the necessary output data for a more accurate estimation of the electronic properties of complex structures [19].

Additionally, DFT is one of the important methods that demonstrated a great advantage over Hartree-Fock [21]. DFT is frequently employed for several different reasons, which is quicker than other Post Hartree-Fock methods and often produces the greatest efficiency [22, 23]. In this present study, Density Functional Theory

(DFT) was utilized in the investigation to calculate HOMO and LOMO states for 2-Nitrophenol $\text{C}_6\text{H}_5\text{NO}_3$ using several different base sets (6-31G, 6-311G, 3-21G, SSD, cc-pVDZ, cc-pVTZ, LanL2MP, LanL2DZ, and STO-3G) to determine the band gap (BGs) of the compound. Classifications of electronic properties were discovered by using structures that had their shape optimized. Parameters were determined for the following properties: total energy ΔE , electronegativity (χ), dipole moment (Debye), softness (S), hardness (η), chemical potential (μ), Chemical potential (Pi), and electrophilicity (ω).

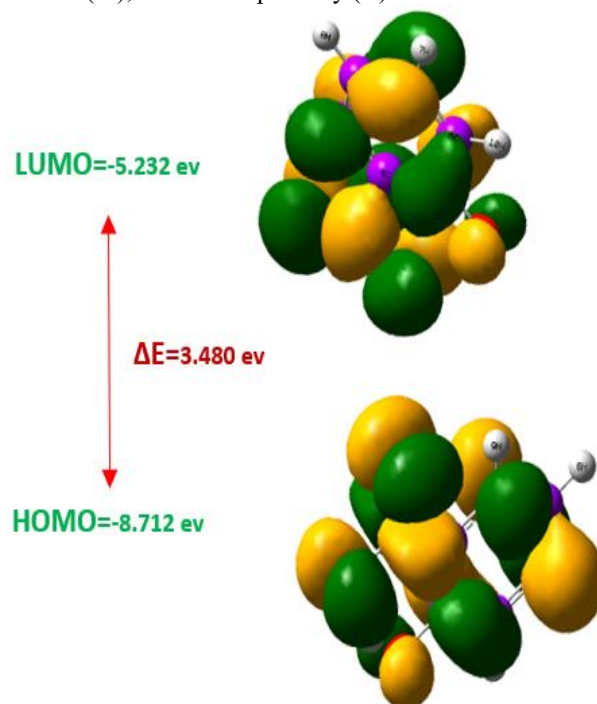


Figure 2 The HOMO=36, and LUMO=37 MOs of 2-NP molecules with 3-21G basis set, and B3LYP of DFT

3. RESULTS AND DISCUSSIONS

3.1. Geometry Optimization

Figure 1 shows the calculated ground energies for the optimized 2-Nitrophenol ($\text{C}_6\text{H}_5\text{NO}_3$) molecules. To achieve more complex geometry enhancements, B3LYP/6-31G base sets were utilized. However [24], some techniques, including (Molecular Mechanics method, Density Functional Theory (DFT), and Hartree-Fock techniques) are employed to optimize a compound structure. But in this present study DFT technique has been used to optimize the $\text{C}_6\text{H}_5\text{NO}_3$ structure. A beneficial geometry optimization method for this approach first determines the energy associated with a specific starting molecule shape [24].

3.2. computed electron structure

The optimal geometry was created when running the Gaussian software with the DFT, as illustrated in Figure 1. In the 2-Nitrophenol structure, there is six carbon bond (1C, 2C, 3C, and 6C) that bonds with four hydrogen atoms (7H, 8H, 9H, and 10H), and 4C with a nitrogen bond (12N). Also, 5C has an oxygen bond with (11O). The fourth carbon has a single bond with 12N, while 12N has one bond with 14O, and a double bond with 13O.

Molecules have unique orbitals, different from the orbitals observed in atoms. The kind of molecule that it is

may be determined by the amount of band gap (BG) energy that is different between (HOMO) and (LUMO). In this work, numerous different values of BG energy have been evaluated for each basis set. The smallest amount of BG energy is 3.48 eV in a 3-21G base set for HOMO=36, and LUMO=37 molecular orbital (MO). The huge value of BG indicates that this molecule is more stable than others. However [25], DFT processes are often faster than those of the other methods such as Hartree-Fock method, while still producing the same results.

DFT was used to compute the electron density in addition to other electronic parameters and the structure such as E_{LUMO} , E_{HOMO} , total energy ΔE , electronegativity (χ), hardness (η), softness (σ), electrophilicity index (ω), nucleophilicity index (ϵ), Chemical potential (Pi), and dipole moment (μ). The LUMO, HOMO, and μ values of the compound are computed in Gaussian using the output data, whilst the values of the other parameters are found via the use of standard formulas [25]. The electron affinity (A), and ionization potential (I) of the molecule are shown in equations (1), (2):

$$A = -E_{LUMO} \quad (1)$$

And

$$I = -E_{HOMO} \quad (2)$$

Data from **Table 2** reveals a difference between the I and A values of 2-Nitrophenol. Moreover, as shown by Koopmans' theory, E_{HOMO} and E_{LUMO} values and electron affinity values of every molecular kind are related to the ionizing energy state. Koopmans' principle says that the HOMO's negative energy value is equal to a molecule's first ionization energy [26, 27]. The following equation (3) was used to determine the energy BG, denoted by the symbol ΔE :

$$\Delta E = E_{LUMO} - E_{HOMO} \quad (3)$$

The value of the energy BG is high, which indicates that this molecule has a higher degree of stability. It is possible to analyze the stability of the ($C_6H_5NO_3$) molecule and its chemical reactivity by using the energy BG between the HOMO and LUMO orbitals. However [28], the equation provides a foundation for making a theoretical determination of the electronegativity (χ), molecular softness (σ), and hardness (η) as shown in equations (4), (5), and (6):

$$\chi = (I + A) / 2 \quad (4)$$

$$\eta = (I - A) / 2 \quad (5)$$

$$\sigma = 1/\eta \quad (6)$$

Using the relevant equations shown below, we were able to determine the values of Chemical potential (Pi), and dipole moment (μ) as shown in equations (7), (8) [19]:

$$Pi = -\chi \quad (7)$$

$$\mu = - (I + A) / 2 \quad (8)$$

as may be seen in equations (9), and (10) below: Pi and η are also connected to the nucleophilicity (ϵ), and electrophilicity (ω) indexes, respectively:

$$\omega = Pi^2 / \eta^2 \quad (9)$$

$$\epsilon = Pi \times \eta \quad (10)$$

The ω index measures the amount of energy that is wasted as a result of the whole energy transfer that occurs between receivers and transmitters [29]. Also the nucleophilicity index is the new identity for the chemical composition [21]. In this study, DFT has seen significant use in predicting molecules' characteristics and providing theoretical explanations in various chemistry-related areas. The electronic and molecular structural characteristics of the 2-Nitrophenol for ($C_6H_5NO_3$) substances are shown in **Table 2**. The LUMO, and HOMO energy values suggested the existence of an overarching pattern among the various basis set that was investigated. However, the BG energy of 2-Nitrophenol was evaluated experimentally in the past at a wavelength of 350, and 400 nm is 3.54 eV and 3.10 eV. This result is in total agreement compared to our theoretical finding. These findings are in complete accord with the results of our theoretical investigation [30]. According **Table 1** to our theoretical findings of this research, the 3-21G basis set has the lowest energy BG 3.48 eV compared to other basis sets evaluated by LUMO, and HOMO levels. Soft molecules are described as those having a small energy gap between HOMO and LUMO levels. In the quantum chemical process, electronegativity (χ), electronic, and molecular chemical potential (Pi) are significant factors. When the value of electronegativity is raised, atoms and molecules have a larger capacity to attract electrons to themselves, while the lower stability and increased reaction are associated with higher chemical potential values. For example, in this present study 3-21G basis set has a larger capacity $\chi=5.972$ eV to attract electrons. When investigating the physicochemical characteristics of compounds, the electrophilicity ω index magnitude is an important chemical composition description. More reactionary nucleophilicity (ϵ) is assumed to have a smaller value of (ω) than a large and powerful electrophile with such a great value of (ω). **Table 2** has been shown when ω value increased with the ϵ value decreased.

In this present study, the highest hardness (η) and softness (σ) of 2-Nitrophenol for ($C_6H_5NO_3$) were found in the 3-21G basis set. This result is relevant to a lower band gap energy at the same basis set (3-21G, BG= 3.480 eV, $\eta=1.740$ eV, and $\sigma= 0.574$ eV⁻¹). dipole moment (μ) exists when chemically related molecules have different electronegativity χ . In addition, the magnitude of the dipole moment is dependent on the big value of the compound's BG. As an example, in comparison to other basis sets, the LanL2MP and STO-3G basis sets have the highest BGs and dipole moments.

3.3. The density of states calculations (DOS)

One of the most important aspects that decides certain spectroscopy, optical behavior, and electrical characteristics, such as UV spectra and chemical bonding, is the atomic molecular orbital theory [31]. In a quantum mechanical system, the electronics DOS is a measurement that determines how "packed" electrons'

Table 1 BGs energy with various basis set for 2-NP DFT

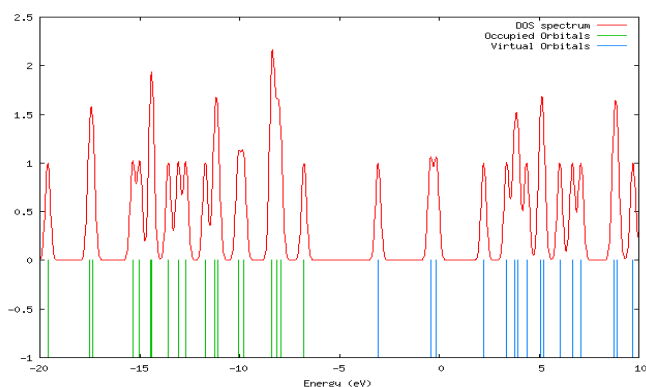


Figure 3 DOS for 2-NP with 3-21G basis set, and B3LYP

densities are in different energy states. However, only DOS to 3-21G basis set has been computed in this part. It is possible to use the formula to compute the DOS as a function of energy levels as shown in equations (11) [32]:

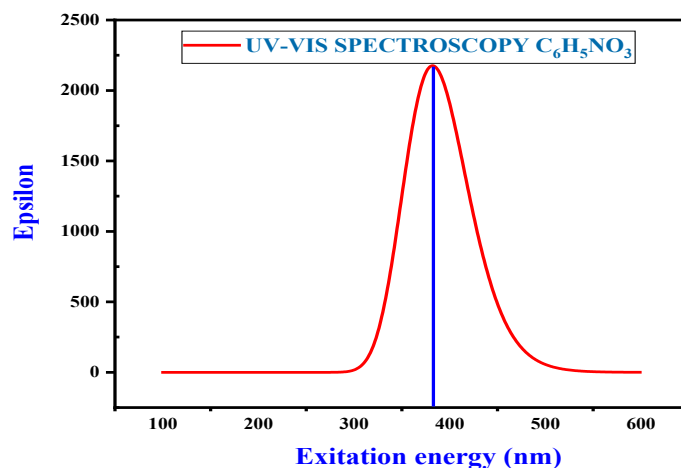
$$\text{DOS}(E) = \sum g(E - \epsilon_i) \quad (11)$$

Where E = total electron energy, g is a Gaussian function that has a constant FWHM = 0.3, and The value of ϵ_i denotes the energy of the i^{th} orbitals. During the calculations, a suitable DFT was used so that an exact evaluation could be obtained of the BG=3.48 eV of the 3-21G basis set. There were found to be 100 different molecular orbital symmetries in the 2-NP structure [33, 34]. The highest value of DOS for 2-NP was investigated 2.23 eV/atom, and the energy range was from -20 eV to 20 eV as shown in **Figure 3**. Also, as can be shown in Table 1, the BGs values have been measured for all basis sets of 2-NP has both decreased and increased because of the absence of electronegativity, electron affinity, and μ . According to this finding, the energy level of components will affect electronic density. When there are more nuclei in an atom, the possibility of splitting rises because some of the nuclei's spin orbits overlap with one [32, 33].

Figure 4 UV Spectroscopy of 2-NP with RB3LYP/TD-FC with 3-21G basis set, and DFT method

Table 2 Molecular parameters of 2-NP parameters in DFT

| Basis set | HOMO/eV | LUMO/eV | ΔE /eV |
|-----------|----------|----------|----------------|
| 6-31G | -7.02024 | -3.46019 | 3.560054 |
| 6-311G | -7.22487 | -3.67108 | 3.553796 |
| 3-21G | -8.71279 | -5.23273 | 3.480053 |
| SSD | -7.23004 | -3.69203 | 3.538013 |
| cc-pVDZ | -6.94514 | -3.24386 | 3.701281 |
| cc-pVTZ | -7.13426 | -3.47869 | 3.655566 |
| LanL2MP | -4.32823 | -0.10504 | 4.223194 |
| LanL2DZ | -7.23412 | -3.6991 | 3.53502 |
| STO-3G | 4.32823 | -0.10504 | 4.223194 |



| Basis set | UNIT | DFT | | | | C ₆ H ₅ NO ₃ | | | | |
|---------------------------------|------------------|-------|--------|-------|-------|-----------------------------------------------|---------|--------|---------|--------|
| | | 6-31G | 6-311G | 3-21G | SSD | cc-pVDZ | cc-pVTZ | P | LanL2DZ | STO-3G |
| Ionization potential (I) | eV | 7.020 | 7.224 | 8.712 | 7.230 | 6.945 | 7.134 | 4.328 | 7.234 | 4.328 |
| Electron affinity (A) | eV | 3.460 | 3.671 | 5.232 | 3.692 | 3.243 | 3.478 | 0.105 | 3.699 | 0.105 |
| Electronegativity (χ) | eV | 5.240 | 5.447 | 5.972 | 5.461 | 5.094 | 5.306 | 2.216 | 5.466 | 2.216 |
| Chemical potential (Pi) | eV | -5.24 | -5.447 | -6.97 | -5.46 | -5.094 | -5.306 | -2.220 | -5.467 | -2.220 |
| Molecular hardness (η) | eV | 1.780 | 1.776 | 1.740 | 1.769 | 1.850 | 1.827 | 2.111 | 1.767 | 2.111 |
| Molecular softness (σ) | eV ⁻¹ | 0.561 | 0.562 | 0.574 | 0.565 | 0.540 | 0.547 | 0.473 | 0.565 | 0.473 |
| Dipole moment (μ) | Debye | -5.24 | -5.447 | -6.97 | -5.46 | -5.094 | -5.306 | -2.220 | -5.467 | -2.220 |
| Electrophilicity (ω) | eV | 8.667 | 9.400 | 16.06 | 9.530 | 7.580 | 8.430 | 1.102 | 9.570 | 1.102 |
| Nucleophilicity (ϵ) | eV | -9.33 | -9.680 | -12.1 | -9.66 | -9.430 | -509.69 | 900 | -9.562 | 300 |

3.1. IR Spectroscopy Analysis

The findings of the IR measurements performed on 2-NP are shown in **Figure 5**, and the B3LYP method using the basis set 3-21G was used to make predictions about the vibrational frequencies of our materials for C-H group. According to the IR findings, the C-H stretching vibration peak was detected between 3209.21 to 3259.55 cm⁻¹ for C₆H₅NO₃ structure. The molecule illustration was constructed with the help of the vibrational band classifications [25, 35].

The results of 2-NP's Raman spectra are shown in **Figure 7**. The maximum frequency peak was observed at 3243.93 cm⁻¹ point, while, in the IR result the maximum frequency peak was seen at 1297.59 cm⁻¹ point. The range of Raman activity was 4.11 to 4.71 to 75 to 111 to 111.86.

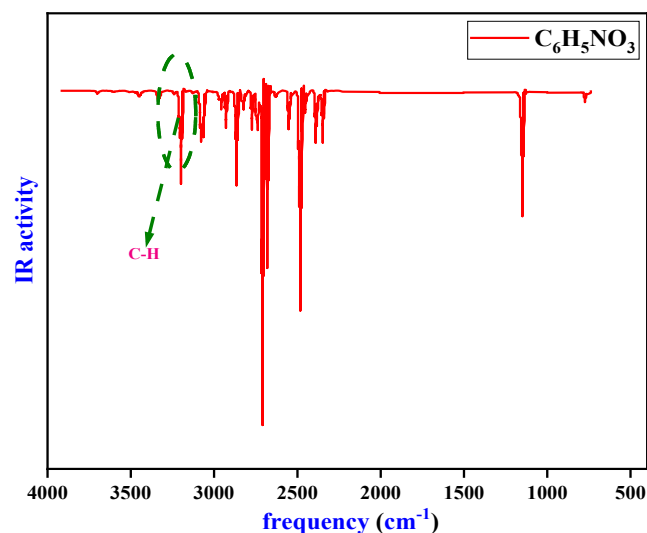
3.2. UV Spectroscopy

UV spectroscopy is a common technique for analyzing compounds, both qualitatively and quantitatively, and for determining their structures [36]. In this present study has been using DFT method, and calculation method RB3LYP/ TD-FC with 3-21G basis set. However, the theoretical findings of UV spectroscopy performed on 2-NP are shown in **Figure 4**. Also, the maximal excitation energy was investigated at a wavelength of 382.1 nm, and the oscillator strength was measured at 0.0537 UV Spectroscopy of 2-NP.

3.3. Potential Energy (PE) Map

The potential energy map plays an essential part in the description of the orientation of the structure of molecule, as well as in the determination of the molecules' optical and **Figure 5** IR spectroscopy of 2-NP, with RB3LYP/ TD-FC with 3-21G basis set, and DFT method electrical characteristics. Because compared C, electronegative of O more then. In **Figure 6**, the majority of the atom's electrons are located in the blue region of the atom, which represents O [31]. Higher electron affinity, dipole moment, and electronegativity are some variables that can influence the Potential Energy Map. The electron affinity of C more than those of both H and O (C= 153.9 kJ/mol > O=141 kJ/mol > H= 72.8 KJ/mol) [37].

Actually, the electrostatic potential map consists electronic density (ρ), and electrostatic potential (EP) or (PE map= ρ



+EP). The density of electrons (ρ) is the number of electrons per unit volume in a given region of space and is a measure of the probability of their particle location [38]. The electrostatic potential is the energy of attraction between a positive unit charge and a distribution of electrons charge or molecules [39]. When discussing electronic density and molecular orbital theory in this diagram, a rise in red implies a higher density of electrons, while a drop in blue suggests a lower density [40].

In the current investigation, the electron density is demonstrated to increase when the color is changed from blue color to red color in the range of $-4.442e^{-2}$ to $4.442e^{-2}$, as seen in **Figure 6**. majority of the atom's electrons are located in the blue region of the atom, which represents oxygen [31].

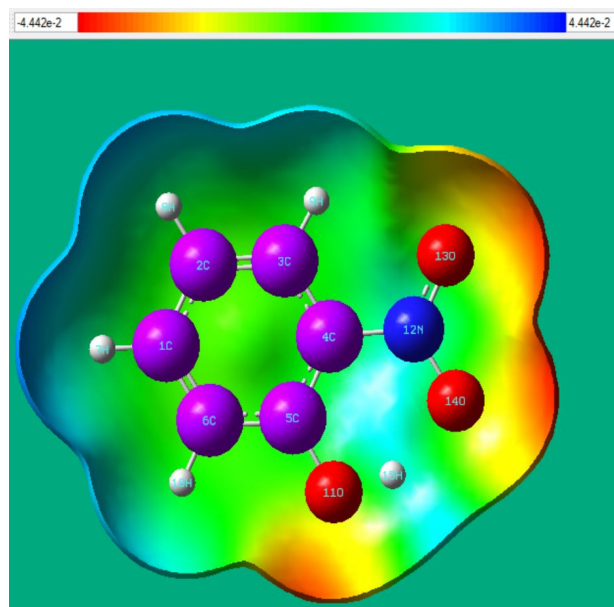


Figure 6 Potential energy (PE) maps of 2-NP, with RB3LYP / 3-21G basis set, and DFT method

4. CONCLUSIONS

In this present study some of the physical, and chemical behavior of 2-nitrophenol (2-NP, $C_6H_5NO_3$) has been investigated including (HOMO, LUMO, DOS, UV, IR spectra, and potential energy map) by using the Gaussian 5.0 software, and DFT method. The smallest BG energy is 3.48 eV in a 3-21G/ B3LYP base set. The DOS for 2-NP was measured to have its maximum possible value of 2.0 eV/atom. According to the results of the IR, and Raman spectrum, the C-H stretching vibration peak for 2-NP was found to be between 3209.21 cm^{-1} to 3259.55 cm^{-1} . The maximum excitation energy was analyzed at a wavelength of 382.1 nm, and the oscillator strength was determined at 0.0537 UV Spectroscopy of 2-NP. Finally, the potential energy map (PEM), the colors are changed from blue to red in the range of $-4.442e^{-2}$ to $4.442e^{-2}$.

Figure 7 Raman spectroscopy of 2-NP, with RB3LYP/3-21G basis set, and DFT method

REFERENCES

- [1] Wu, J.T., Zhang, J.G., Yin, X., He, P., and Zhang, T.L. (2014). Synthesis and Characterization of the Nitrophenol Energetic Ionic Salts of 5, 6, 7, 8-Tetrahydrotetrazolo [1, 5-b][1, 2, 4] triazine, *European Journal of Inorganic Chemistry*, 2014 (27), pp: 4690-4695.
- [2] Allen, S.J., Koumanova, B., Kircheva, Z., and Nenkova, S. (2005). Adsorption of 2-nitrophenol by technical hydrolysis lignin: kinetics, mass transfer, and equilibrium studies, *Industrial & engineering chemistry research*, 44 (7), pp: 2281-2287.
- [3] Aamir, M., Khan, M.D., Sher, M., Bhosale, S.V., Malik, M.A., Akhtar, J., and Revaprasadu, N. (2017). A facile route to cesium lead bromoiodide perovskite microcrystals and their potential application as sensors for nitrophenol explosives, *European Journal of Inorganic Chemistry*, 2017 (31), pp: 3755-3760.
- [4] Reichelt, H., Faunce, C.A., and Paradies, H.H. (2015). Structures of the 2-nitrophenol alkali complexes in solution and the solid state, *The Journal of Chemical Physics*, 143 (4), pp: 044307.
- [5] Ko, J.W., Park, S.H., Jeon, S., Chung, H., and Ko, W.B. (2022). Catalytic activity of C60 fullerene nanowhisker-silver nanoprism composite for reduction of 2-nitrophenol, *Fullerenes, Nanotubes and Carbon Nanostructures*, 30 (5), pp: 584-588.
- [6] Baysal, G., Uzun, D., and Hasdemir, E. (2020). The fabrication of a new modified pencil graphite electrode for the electrocatalytic reduction of 2-nitrophenol in water samples, *Journal of Electroanalytical Chemistry*, 860 113893.
- [7] Kupeta, A., Naidoo, E., and Ofomaja, A. (2018). Kinetics and equilibrium study of 2-nitrophenol adsorption onto polyurethane cross-linked pine cone biomass, *Journal of Cleaner Production*, 179 191-209.
- [8] Buemi, G. (2002). Ab initio DFT study of the rotation barriers and competitive hydrogen bond energies (in gas phase and water solution) of 2-nitroresorcinol, 4, 6-dinitroresorcinol and 2-nitrophenol in their neutral and deprotonated conformations, *Chemical physics*, 282 (2), pp: 181-195.
- [9] Balakrishnan, A., Gaware, G., and Chinthala, M. (2022). Heterojunction photocatalysts for the removal of nitrophenol: A systematic review, *Chemosphere*, 136853.
- [10] Assi, N., Mohammadi, A., Sadr Manuchehri, Q., and Walker, R.B. (2015). Synthesis and characterization of ZnO nanoparticle synthesized by a microwave-assisted combustion method and catalytic activity for the removal of ortho-nitrophenol, *Desalination and Water Treatment*, 54 (7), pp: 1939-1948.
- [11] Zhao, K., Wang, J., Kong, W., and Zhu, P. (2020). Facile Green synthesis and characterization of copper nanoparticles by aconitic acid for catalytic reduction of nitrophenols, *Journal of Environmental Chemical Engineering*, 8 (2), pp: 103517.
- [12] Arasteh, R., Masoumi, M., Rashidi, A.á., Moradi, L., Samimi, V., and Mostafavi, S. (2010). Adsorption of 2-nitrophenol by multi-wall carbon nanotubes from aqueous solutions, *Applied Surface Science*, 256 (14), pp: 4447-4455.
- [13] Pauletto, P., Moreno-Pérez, J., Hernández-Hernández, L., Bonilla-Petriciolet, A., Dotto, G., and Salau, N. (2021). Novel biochar and hydrochar for the adsorption of 2-nitrophenol from aqueous solutions: An approach using the PVSDM model, *Chemosphere*, 269 128748.
- [14] Sellaoui, L., Silva, L.F., Badawi, M., Ali, J., Favarin, N., Dotto, G.L., Erto, A., and Chen, Z. (2021). Adsorption of ketoprofen and 2-nitrophenol on activated carbon prepared from winery wastes: A

- combined experimental and theoretical study, *Journal of Molecular Liquids*, 333 115906.
- [15] Dalla Nora, F.B., Lima, V.V., Oliveira, M.L., Hosseini-Bandegharai, A., de Lima Burgo, T.A., Meili, L., and Dotto, G.L. (2020). Adsorptive potential of Zn–Al and Mg–Fe layered double hydroxides for the removal of 2–nitrophenol from aqueous solutions, *Journal of Environmental Chemical Engineering*, 8 (4), pp: 103913.
- [16] Adeosun, W.A., Asiri, A.M., and Marwani, H.M. (2020). Sensitive determination of 2-nitrophenol using electrochemically deposited polymethyl red film for healthcare and environmental safety, *Synthetic Metals*, 261 116321.
- [17] Li, J., He, L., Jiang, J., Xu, Z., Liu, M., Liu, X., Tong, H., Liu, Z., and Qian, D. (2020). Facile syntheses of bimetallic Prussian blue analogues (K_xM [Fe (CN) 6] · nH₂O, M= Ni, Co, and Mn) for electrochemical determination of toxic 2-nitrophenol, *Electrochimica Acta*, 353 136579.
- [18] Yilmaz, E., Tut, Y., Turkoglu, O., and Soylak, M. (2018). Synthesis and characterization of Pd nanoparticle-modified magnetic Sm₂O₃–ZrO₂ as effective multifunctional catalyst for reduction of 2-nitrophenol and degradation of organic dyes, *Journal of the Iranian Chemical Society*, 15 (8), pp: 1721-1731.
- [19] Rebaz, O., KOPARIR, P., QADER, I., and AHMED, L.J.G.U.J.o.S. (2022). Theoretical Determination of Corrosion Inhibitor Activities of Naphthalene and Tetralin, 1-1.
- [20] QADER, İ.N., MOHAMMAD, A., AZEEZ, Y.H., AGİD, R.S., HASSAN, H.S., AL-NABAWİ, S.H.M.J.J.o.P.C., and Materials, F. Chemical Structural and Vibrational Analysis of Potassium Acetate: A Density Function Theory Study, 2 (1), pp: 23-25.
- [21] Pearson, R.G.J.I.c. (1988). Absolute electronegativity and hardness: application to inorganic chemistry, 27 (4), pp: 734-740.
- [22] Aydoğmuş, Z., Aslan, S.S., Yildiz, G., and Senocak, A.J.J.o.a.c. (2020). Differential Pulse Voltammetric Determination of Anticancer Drug Regorafenib at a Carbon Paste Electrode: Electrochemical Study and Density Functional Theory Computations, 75 (5), pp: 691-700.
- [23] AHMED, L., Rebaz, O.J.J.o.P.C., and Materials, F. (2019). A theoretical study on Dopamine molecule, 2 (2), pp: 66-72.
- [24] Bálint, D. and Jäntschi, L.J.M. (2021). Comparison of molecular geometry optimization methods based on molecular descriptors, 9 (22), pp: 2855.
- [25] AKTAŞ, A.E., Rebaz, O., KOPARIR, M.J.J.o.P.C., and Materials, F. Synthesis, Characterization and Theoretical Anti-Corrosion Study for Substitute Thiazole Contained Cyclobutane Ring, 5 (1), pp: 111-120.
- [26] Plakhutin, B.N. and Davidson, E.R.J.T.J.o.P.C.A. (2009). Koopmans' theorem in the restricted open-shell Hartree– Fock Method. 1. A variational approach, 113 (45), pp: 12386-12395.
- [27] Koopmans, T.J.p. (1934). Über die Zuordnung von Wellenfunktionen und Eigenwerten zu den einzelnen Elektronen eines Atoms, 1 (1-6), pp: 104-113.
- [28] Shahab, H., Husain, Y.J.P.J.o.B., and Sciences, A. (2021). Theoretical Study for Chemical Reactivity Descriptors of Tetrathiafulvalene in gas phase and solvent phases based on Density Functional Theory, 3 (2), pp: 167-173.
- [29] Kiyooka, S.-i., Kaneno, D., and Fujiyama, R.J.T.L. (2013). Parr's index to describe both electrophilicity and nucleophilicity, 54 (4), pp: 339-342.
- [30] Ernst, H.A., Wolf, T.J., Schalk, O., González-García, N., Boguslavskiy, A.E., Stolow, A., Olzmann, M., and Unterreiner, A.-N.J.T.J.o.P.C.A. (2015). Ultrafast dynamics of o-nitrophenol: An experimental and theoretical study, 119 (35), pp: 9225-9235.
- [31] Nasidi, I.I., Kaygili, O., Majid, A., Bulut, N., Alkhedher, M., and Eldin, S.M.J.A.O. (2022). Halogen Doping to Control the Band Gap of Ascorbic Acid: A Theoretical Study.
- [32] Kareem, R.O., Kaygili, O., Ates, T., Bulut, N., Koytepe, S., Kuruçay, A., Ercan, F., and Ercan, I.J.C.I. (2022). Experimental and theoretical characterization of Bi-based hydroxyapatites doped with Ce, 48 (22), pp: 33440-33454.
- [33] Korkmaz, A.A., Ahmed, L.O., Kareem, R.O., Kebiroglu, H., Ates, T., Bulut, N., Kaygili, O., and Ates, B.J.J.o.t.A.C.S. (2022). Theoretical and experimental characterization of Sn-based hydroxyapatites doped with Bi, 1-13.
- [34] Hssain, A.H., Bulut, N., Ates, T., Koytepe, S., Kuruçay, A., Kebiroglu, H., and Kaygili, O.J.C.P.L. (2022). The experimental and theoretical investigation of Sm/Mg co-doped hydroxyapatites, 800 139677.
- [35] Mahmood, B.K., Kaygili, O., Bulut, N., Dorozhkin, S.V., Ates, T., Koytepe, S., Gürses, C., Ercan, F., Kebiroglu, H., and Agid, R.S.J.C.I. (2020). Effects of strontium-erbium co-doping on the structural properties of hydroxyapatite: An Experimental and theoretical study, 46 (10), pp: 16354-16363.
- [36] Edwards, A.A. and Alexander, B.D. (2017). UV-Visible absorption spectroscopy, organic applications.
- [37] Wu, T.-Y.J.P.R. (1955). Electron affinity of boron, carbon, nitrogen, and oxygen atoms, 100 (4), pp: 1195.
- [38] Zhelavskaya, I.S., Shprits, Y.Y., and Spasojevic, M., *Reconstruction of plasma electron density from satellite measurements via artificial neural networks*, in *Machine learning techniques for space weather* 2018, Elsevier. p. 301-327.
- [39] Bort, J.A. and Rusca, J.B., (2007). *Theoretical and computational chemistry: foundations, methods and techniques*, Publicacions de la Universitat Jaume I,

[40] Yu, F., Li, J., Liu, Z., Wang, R., Zhu, Y., Huang, W., Liu, Z., and Wang, Z.J.J.o.C.S. (2022). From

Atomic Physics to Superatomic Physics, 1-18.